

Failure Paths Analyses of the Leadframe/EMC System

H. Y. Lee* and S. R. Kim**

*Dept. of Materials Science and Engineering, Korea Advanced Institute of Science and Technology,
373-1 Kusong-dong, Yusong-gu, Taejon 305-701, Korea

E-mail : hoyoung@kaist.ac.kr

**Senior Scientist, Polymeric Materials Gr., Sam Yang Central R&D Center,
63-2 Hwaam-dong, Yusong-gu, Taejon, 305-348 Korea

E-mail : srkim@samyang.co.kr

Abstract : Copper-based leadframe sheets were oxidized in a black-oxide forming solution, and molded with epoxy molding compound (EMC) to form sandwiched double-cantilever beam (SDCB) specimens. The adhesion strength of leadframe/EMC interface was measured in terms of fracture toughness by using SDCB specimens and the fracture surfaces were analyzed by various equipments such as glancing-angle XRD, AFM, and SEM. Results showed that three types of failure paths, which were closely related to the surface condition of leadframes before molding.

1. Introduction

Popcorn cracking phenomena have been a major package reliability issue for the surface mount IC packages, especially when die-pad sizes were large.¹⁾ Package cracking occurs in different modes depending on the package geometry, materials, processes, and failure generally occurred at the weakest interface.^{1,2)} Delamination of the die-pad/EMC (epoxy molding compound) interface is cited as one of the most frequent failure reasons^{3,4)} and the procurement of a strong leadframe/EMC interface is regarded as a key solution to prevent the delamination.^{5,6)}

In this work, the black-oxide layer was introduced on the surfaces of Cu-based leadframe, and the fracture toughness of the leadframe/EMC interface was measured by using sandwiched double-cantilever beam (SDCB) specimens, which were followed by the fractographic analyses on the basis of XRD, AFM and SEM analyses.

2. Experimental Procedure

2.1 Formation of Black Oxide

Copper-based leadframes (commercial name: EFTEC-64T) with the nominal composition of Cu-

0.3Cr-0.25Sn-0.2Zn and the thickness of 0.15 mm were used. Organic impurities on the leadframe surfaces were removed by ultrasonic cleaning in acetone for 20 minutes and subsequently native oxides were removed by pre-treatment solution (commercial name: Activan #6, a brand of Han Yang Chemical Ind., Korea). After the pre-cleaning, leadframe sheets were immersed in a hot alkaline solution to form a black-oxide layer on the surface.⁷⁾ The oxidation times were typically less than 20 minutes. The black-oxide layer was analyzed by SEM, TEM and glancing-angle X-ray diffractometer (XRD). Then, the oxide thickness was measured by the galvanostatic reduction method,⁸⁻¹⁰⁾ which is described in detail in the reference.⁸⁾

2.2 Preparation of SDCB Specimens and Mechanical Tests

After the oxidation treatments, leadframe sheets were compounded with EMC (oxygen-carbon-nitrogen type, DMC-20 by Dong-Jin Chemical Co., Korea) in a compression molding system for 15 minutes at 175°C and then machined into SDCB specimens for the fracture toughness testing. After the machining, all specimens were post-cured at 175°C for 4 hours.

The fracture toughness or critical energy-release rate, G_{IC} was calculated from equation (1) on the basis of the reference;¹¹⁾

$$G_{IC} = \frac{P_c^2 a^2}{t^2 t^3 E} \left[3.467 + 2.315 \left(\frac{l}{a} \right) \right]^2 \quad (1)$$

where, P_c is the critical load, E is the plane strain tensile modulus defined by $E/(1-\nu^2)$ (E : Young's modulus, ν : Poisson's ratio), a is the crack length, t is the specimen thickness, and l is the specimen half-height, respectively. A sandwiched specimen can be regarded as homogeneous specimen when the inserted layer is sufficiently small compared to the other specimen geometry.¹²⁾

3. Results and Discussion

3.1 Oxidation Characteristics

3.1.1 Microstructure

Surface morphologies of oxidized leadframe were examined by secondary electron microscope.¹³⁾ There was no remarkable feature in pre-cleaned surface, but smooth pebble-like precipitates formed only after few seconds and coarsened to the average size of 0.2 μm after 0.5~1.0 minute. The pebble-like precipitates with smooth facets were later identified as Cu_2O . Then, acicular oxide precipitates, 0.5~1.0 μm in length, started to nucleate atop the Cu_2O layer approximately after one minute, and more or less patch over the whole surface after two minutes. Through the glancing-angle XRD analyses, the newly formed precipitates were confirmed as CuO . With further oxidation, the CuO layer thickened and became dense, but the size of the forefront CuO needles remained more or less constant.

3.1.2 Thickness

The thickness of oxide layers were measured by using galvanostatic reduction method⁸⁻¹⁰⁾ in which the copper oxide is electrochemically reduced under constant current density.¹³⁾ The initially formed Cu_2O layer grew to the average thickness of around 200 nm till one minute. However, the CuO layer, which appeared after one minute, grew parabolically with oxidation time, and reached 1300 nm at 20 minutes.

3.2 Fracture Toughness

3.2.1 SDCB Tests

Fracture toughness of leadframe/EMC interface was measured by using SDCB specimens,¹³⁾ and the results are showed that the untreated leadframe/EMC interface showed almost no adhesion, and this was remained so up to one minute. However, when the leadframe surface was covered with acicular CuO , the fracture toughness increased rapidly up to $G_{IC}=80 \text{ J/m}^2$ after two minutes and reached the saturation value of $G_{IC}=100 \text{ J/m}^2$ after ten minutes. It was found from the results that the presence of pebble-like Cu_2O crystals with smooth facets played no role in the adhesion to EMC thereby provided no fracture resistance to the quasi-mode I loading, while acicular CuO crystals enhanced fracture resistance. This might be attributable to that the adhesion between Cu-based leadframe and EMC occurs by mechanical interlocking of CuO needles into epoxy resin.

3.2.2 Adhesion Mechanism

The cross-sectional TEM image was taken from twenty-minute-oxidized leadframe sheet and shown in Fig. 1. The CuO needles and the gap among the CuO needles are found. The real length of CuO needles is estimated at more than 2 μm on the basis of this TEM



Fig. 1. Cross-sectional TEM micrograph of twenty-minute-oxidized leadframe.

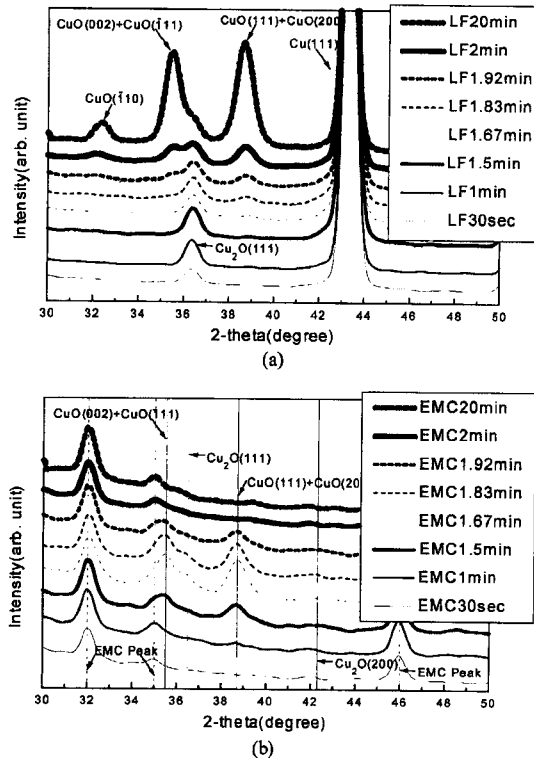


Fig. 2. Glancing-angle X-ray diffraction patterns out of fracture surface of separated (a) leadframe side and (b) EMC side.

micrograph. Comparing between the average thickness of CuO layer measured by galvanostatic reduction method, 1.3 μm , and real length of CuO needle, 2~3 μm , it becomes clear that most part of CuO layer is filled with void or gap. Such a void or gap might play an important role in the penetration of epoxy resin, that is why the mechanical interlocking is achieved between CuO needles and epoxy resin during the molding process.

3.3 Failure Path

3.3.1 X-ray Analyses

After the fracture toughness testing, separated leadframe and EMC sides were analyzed by using glancing-angle XRD, and the results are presented in Fig. 2. As can be seen in Fig. 2 (a), the overall trend of separated leadframe side seems to be the same as that of as-oxidized leadframe,¹³⁾ but there were some differences. For example, after two minutes, the height

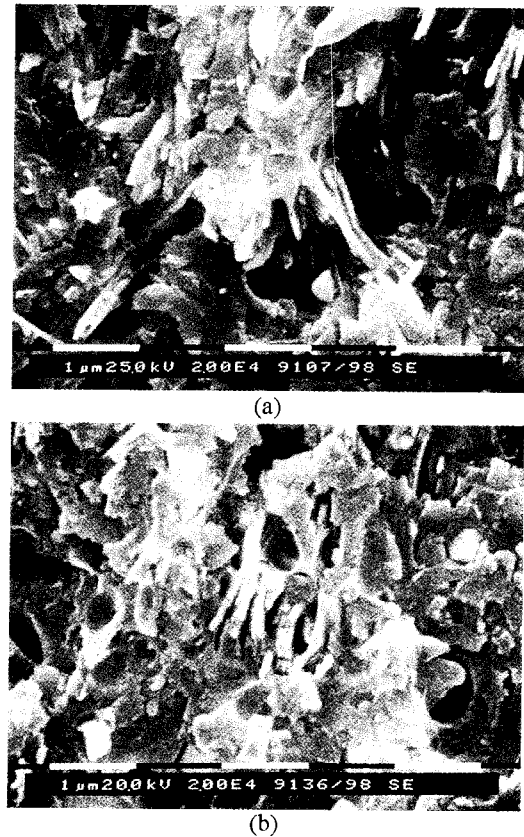


Fig. 3. SEM micrographs out of separated (a) leadframe side and (b) EMC side, where the leadframe was oxidized for 2 minutes before molding.

of the CuO(111)+CuO(200) peak was higher than that of the Cu₂O (111) peak for the as-oxidized leadframe, while the opposite was true for the leadframe side. On the other hand, X-ray analyses on the separated EMC side revealed that there were only EMC peaks till 30 seconds and the CuO peak began to appear at one minute and kept increasing till 1.83 minutes, but finally decreased. This might be ascribed to the detachment of CuO whiskers from the leadframe surface. It can be confirmed from Fig. 3, which shows the traces of broken CuO whiskers on the separated leadframe side and embedded CuO whiskers on the separated EMC side.

3.3.2 AFM Analyses

AFM analyses were carried out on the as-oxidized leadframe and the separated leadframe and EMC surfaces. The results are shown in Fig. 4. In case of as-

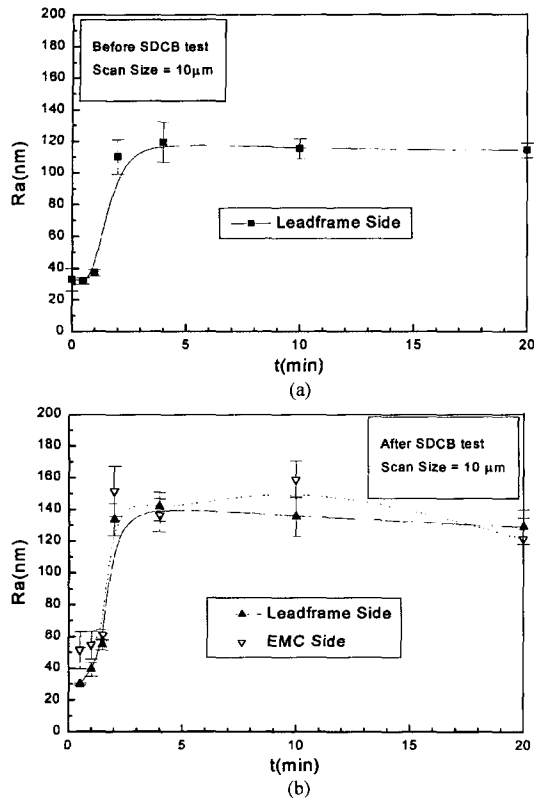


Fig. 4. Variations of average roughness of leadframe with oxidation time (a) before molding and (b) after SDCB test.

oxidized leadframe, since Cu_2O has a smooth facets,¹³⁾ the average roughness was relatively low when Cu_2O was dominant on the leadframe surface. However, when CuO was dominant on the leadframe surface, the average roughness was relatively high. This may be due to the acicular shape of CuO .¹³⁾ Such a roughness change with the surface state of leadframe was well preserved in case of separated leadframe. Comparing between as-oxidized and separated leadframes, one can readily find out that there is almost no difference in roughness. Such a good agreement may be ascribed to the similar nature of fracture surface.

3.3.3 SEM Analyses

The fracture surfaces were examined by using SEM, and results are shown in Fig. 5. The surface morphologies of separated leadframe which were oxidized for 30 seconds before molding are very similar to that of as-oxidized leadframe surface. For that reason, the surface roughness was relatively low and almost the

same as compared to that of as-oxidized leadframe. Such smooth morphologies were well preserved till 1.83 minutes. However, when the oxidation time was more than two minutes, the surface morphologies were abruptly changed so the morphologies were much rougher than to be seen. The measured roughness was relatively high and also almost the same as compared to that of as-oxidized leadframe. The reason why the average roughness of separated leadframes of which oxidation time was more than two minutes was high might be ascribed to that the failure was occurred near CuO/EMC interface.

3.3.4 Failure Paths

From the above good agreement among X-ray, AFM and SEM results, fracture paths can be presumed to be the same as follows ; in case of $t < 2$ minutes, fracture may occur at the $\text{EMC}/\text{Cu}_2\text{O}$ ($t < 1$ minute) or $\text{CuO}/\text{Cu}_2\text{O}$ ($1 \leq t < 2$ minutes) interface, and consequently Cu_2O is left on the separated leadframe side so that the average roughness becomes nearly the same as that of as-oxidized leadframe. In case of $t \geq 2$ minutes, fracture may occur near the EMC/CuO interface. The failure paths can be schematically delineated with oxidation time as shown in Fig. 6.

4. Conclusions

1. The fracture toughness of the leadframe/EMC interface was nearly zero for the untreated interface, and remained so for the $\text{Cu}_2\text{O}/\text{EMC}$ interface. However, once continuous CuO layer formed on the Cu_2O layer, fracture toughness increased to 80 J/m^2 after two minutes and reached the saturation value of 100 J/m^2 after ten minutes.

2. Acicular CuO precipitates contribute to the increase of adhesion strength, while smooth-faceted Cu_2O played no role, which can be primarily ascribed to the acicular morphologies of CuO which can interlock epoxy mechanically.

3. Failure paths of SDCB specimens were strongly dependent on the surface state of leadframe before molding. Fracture occurred near the $\text{EMC}/\text{Cu}_2\text{O}$ ($t < 1$ minute) or the $\text{CuO}/\text{Cu}_2\text{O}$ interfaces ($1 \leq t < 2$). For $t \geq 2$ minutes, failure occurred inside EMC near the EMC/CuO interface.

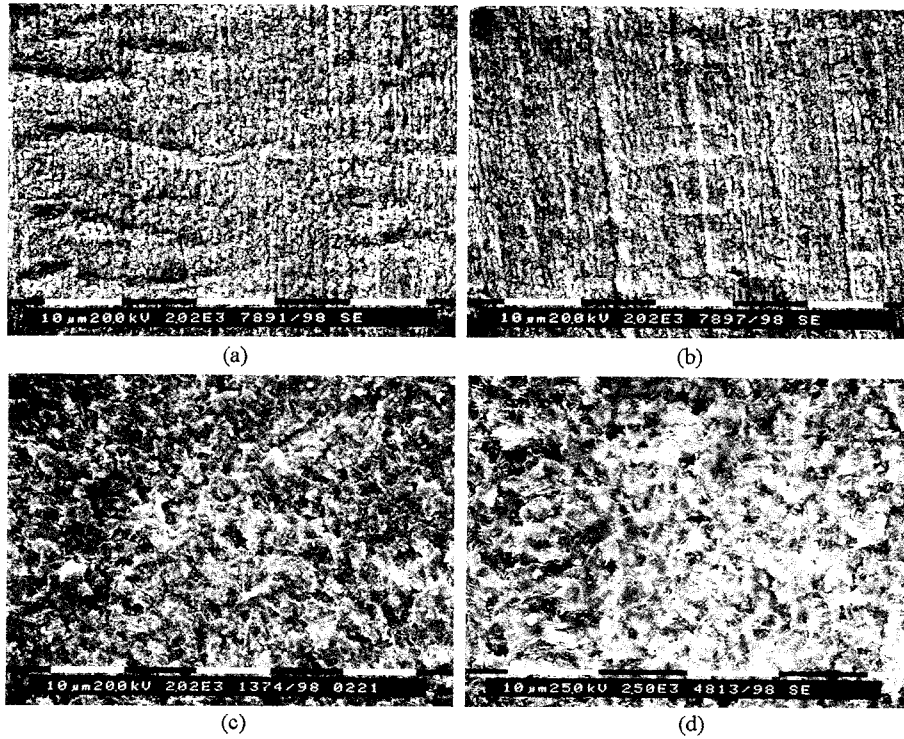


Fig. 5. SEM micrographs out of separated leadframe sides: The oxidation times of leadframes before molding are (a) 30 seconds, (b) 1 minute 50 seconds, (c) 2 minutes, and (d) 20 minutes.

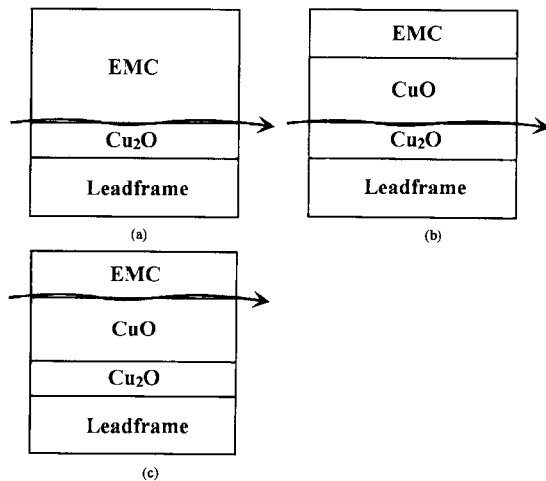


Fig. 6. Schematic diagrams of failure paths with oxidation time: (a) is for the oxidation time $t < 1$ minute, (b) is for $1 \leq t < 2$ minutes and (c) is for $t \geq 2$ minutes.

References

1. T. C. Chai, K. C. Chan, E. H. Wong, X. J. Fan, and

T. B. Lim, in Proceeding of the 49th Electronic Components and Technology Conference, San Diego, California U.S.A., May 702 (1999).
 2. E. H. Wong, Y. C. Teo and T. B. Lim, in Proceeding of the 48th Electronic Components and Technology Conference, Seattle, Washington U.S.A., May 1372 (1998).
 3. M. Kitano, A. Nishimura, S. Kawai and K. Nishi, Proc. Int. Reliab. Phys. Symp., 90 (1988).
 4. G. S. Ganesan and H. M. Berg, IEEE Trans. on CHMT, 16, 940 (1993).
 5. C. Q. Cui, H. L. Tay, T. C. Chai, R. Gopalakrishan and T.B. Lim, in Proceeding of the 48th Electronic Components and Technology Conference, Seattle, Washington U.S.A., May 1162 (1998).
 6. B. H. Moon, H. Y. Yoo and K. Sawada, in Proceeding of the 48th Electronic Components and Technology Conference, Seattle, Washington U.S.A., May 1148 (1998).
 7. H. K. Yun, K. Cho, J. H. An and C. E. Park, J. Mater. Sci., 27, 5811 (1992).
 8. J. R. G. Evans and D. E. Packham, J. Adhesion, 9, 267 (1978).

9. V. Ashworth and D. Fairhurst, *J. Electrochem. Soc.*, 124, 506 (1977).
10. H.-H. Strehblow and B. Titze, *Electrochimica Acta*, 55, 839 (1980).
11. T. S. Oh, R. M. Cannon and R. O. Ritchie, *J. Am. Ceram. Soc.*, 70, C-352 (1987).
12. Z. Suo and J. W. Hutchinson, *Mater. Sci. and Eng.*, A107, 135 (1989).
13. H. Y. Lee and Jin Yu, *J. of the Microelectronics & Packaging Society*, 6(2), 1(1999).